April 30, 2020

PharmacologyOnLine

Archives • 2020 • vol.1 • 213-228

IN-SILICO APPROACH FOR THE IDENTIFICATION OF NEW MOLECULES FOR ALZHEIMER'S DISEASE (AD)

Md. Alamgir Hossain[1]

[1] Department of Pharmacy, Jagannath University, Dhaka, Bangladesh

*alamgir.jnu10@gmail.com

Abstract

Alzheimer's disease (AD) is a malignant neurodegenerative disorder which causes the destruction of brain cells that ultimately results in memory loss and cognitive dysfunction. Deposition of b-amyloid fibril, the formation of b-amyloid oligomers, hyperphosphorylation of tau protein, oxidative stress, low levels of acetylcholine is reported as the main hallmarks of the disease. To date, current therapy is based on cholinesterase inhibition which is mainly symptomatic but the efficacy is limited. Phosphodiesterase-4 (PDE4) is an enzyme that aids in the hydrolysis of cyclic AMP (cAMP). It is divided into four subtypes known as PDE4A, PDE4B, PDE4C, and PDE4D. Recent studies suggest that PDE4 is a promising target for the development of new drugs for various neuronal diseases. In this research, pharmacophore-based virtual screening was done to get prominent molecules for Alzheimer's Disease (AD). After virtual screening and toxicity were checked, 145 molecules remained. The remaining compounds were subjected to molecular docking studies with three docking software. After molecular docking, 21 molecules left and DSX scoring was done for these molecules. Among 21 molecules, 9 molecules got selected after DSX and binding interaction was evaluated for 9 molecules and finally got 3 molecules. Molecular dynamics simulation was performed for these three molecules to check their stability where they showed good performance.

Keywords: *Alzheimer's Disease (AD), Phosphodiesterase-4, Pharmacophore modeling, Virtual screening, Rescoring, Molecular dynamics (MD) simulation*

Introduction

Alzheimer's Disease (AD) is said to be the most common cause of dementia. According to the World Alzheimer's report, about 35.6 million people were suffering from AD in 2010 and there is a possible chance of increasing this number to 65.7 million by 2030 and 115.4 million by 2050 [1].

A number of hormones and neurotransmitters in signal transduction pathways are mediated by cyclic adenosine monophosphate (cAMP) and cyclic guanosine monophosphate (cGMP) which are two well-known intracellular second messengers [2-4]. Phosphodiesterase (PDE), an enzyme which is a member of the families of cyclic nucleotide liable for the breakdown of cAMP or cGMP to 5'-AMP or 5'-GMP [5-7].

Till now, 11 families of PDE4 have been identified (PDE1-PDE11) and they are categorized based on their primary structure, their abundance in tissue and their ability to hydrolyze. Considering the substrate group, PDE families are normally classified in three groups, PDE4, PDE7, and PDE8 are specific to cAMP whereas PDE5, PDE6 and PDE9 are specific for cGMP, On the other hand, PDE1, PDE2, PDE3, PDE10 and PDE11 which are specific for both substrates and hydrolyze both cAMP and cGMP [8-10]. Among all the PDE families, PDE4 is thought to be the most prominent enzyme that which controls the intracellular cAMP [11]. This enzyme is being studied as a prominent target for treating depressive disorder for a long period. Rolipram, a novel inhibitor of PDE4 has shown that there is a relation between PDE4 and animal's reaction sensitive to antidepressant drugs [12]. Later studies revealed the effect of rolipram that showed strong antidepressant activity in various preclinical experiments [13]. Recent researchers have suggested that PDE4 can be a good therapeutic target for other CNS disorder like Alzheimer's disease, Parkinson's disease, Schizophrenia and so on [14-16]. There are about 20 potent inhibitors of PDE4 is available and are using in different diseases [17].

The purpose of this research was to design new molecules for AD through *in-silico* approach. For this, pharmacophore-based virtual screening, molecular docking, rescoring for validation of molecular docking and ADMET analysis and binding interaction was evaluated. Finally, molecular dynamics (MD) simulation was carried out to evaluate the actual stability of the hit compounds. The pharmacophore model of a protein-ligand complex shows the integral interaction characteristics which are liable for inducing or inhibiting biological response [18]. This 3D-pharmacophore model describes the 3D geometric features of a bioactive compound besides its chemical feature. The model is used to retrieve bioactive molecules via virtual screening [19]. Virtual screening is a useful *in-silico* technique for identifying active compounds from the chemical databases [20]. The combination of the pharmacophore model and the virtual screening approach has become a very popular and efficient method for *in-silico* drug discovery process [21]. Normally, the biological activity of a molecule is measured by the affinity of the molecules to the targeted receptor which can easily be determined through *in-silico* approach. For this purpose, molecular docking simulation is used to calculate the binding energy which is a beneficial method to predict the pose of the compounds and select compound for experimental assessment. Two basic steps are involved in the molecular docking approach. One is predicting the multiple structured conformation to the binding pocket and another is scoring the pose to rank conformation [22,23].

Methods

Pharmacophore model and database generation

Here, the pharmacophore model was generated for one PDE4 protein (PDB ID: 1RO6) with the software LigandScout with its default parameters [24]. To validate the model, a small database containing 65 [25] known active PDE4 inhibitors and 106 inactive compounds were generated. The inactive molecules were generated using DUD: E web server [26]. After validating the model, we took the model for virtual screening.

Virtual screening

The pharmacophore model was used against three distinct chemical databases for virtual screening to get the initial hit molecules. The databases are Chembridge library [27], Asinex gold and Asinex-platinum Library [28]. After completing virtual screening, those molecules were taken for further study possessing the minimum pharmacophore fit value that we fixed. Virtual screening was carried out with the software catalyst [29].

Drug likeness filtration

Many compounds get removed from entering the drug development pipeline due to its poor AMDET properties. AMDET properties were focused during getting the hit compounds. Firstly, we filtered those molecules obtained after sorting based on pharmacophore fit value by applying the Rule of Five developed by Lipinski [30] and secondly, by considering several ADMET parameters including Pan Assay Interference Compounds (PAINS). The ADMET was obtained from FAFdrugs4 web server [31].

Protein structure preparation

Crystal structure of our selected protein (PDB ID: 1RO6) was downloaded from the RCSB protein data bank [32]. The attached water molecules and other heteroatoms were removed. Finally, polar hydrogen and Gasteiger charge were added and prepared the protein by using AutoDock Tools 1.5.6 [33].

Ligands preparation

Schrödinger LigPrep application was used to generate 3D coordinates for the ligands available after drug-likeness filtration [34]. The molecules were saved in SDF format to dock with the protein.

Molecular docking and rescoring

Molecular docking was carried out to the active site of the protein. The active site of the protein was GLN A:443, PHE A:446, HIS A:234, TYR A:233, ILE A:410 and PHE A:446. During the docking simulation, the grid box size was X=72.055, Y= 105.177, Z= 70.561, and the center was X=21.7245, Y= 94.2185, Z=34.2975 so that the whole active site is covered. Docking was carried out using PyRx [35], Vega zz [36] and AutoDock vina [37]. Finally, to validate the docking score, the selected ligands were rescored again. This scoring system helped to get the final hit compounds. Rescoring was done by using DrugScoreX online web server [38].

Molecular dynamics simulation

Molecular dynamics simulation was done for the final 2 hit compounds to check the stability of these compounds. YASARA was used in windows 64-bit OS to carry out the simulation [39]. Both complexes were cleaned initially and optimization of hydrogen bonding was done. At constant pressure, the simulation was run for 50 ns. AMBER14 N force field was applied to obtain the parameters of the force field [40-42]. RMSD (Root Mean Square Deviation), RMSF (Root Mean Square

Fluctuation) and Rg (Radius of Gyration) were taken into account to check the relative stability of the ligands in the binding site of the protein [43-45].

Result

The figures below (Figure 1 and Figure 2) represent the pharmacophore features obtained from LigandScout and the 2D structure of the attached ligands. Pharmacophore features are generally expressed by the following method: Yellow-colored sphere represents the hydrophobic feature. On the other hand, red and green arrows represent the hydrogen bond acceptor and hydrogen bond donor groups respectively. And excluded volumes are represented by gray spheres [46].

To validate the pharmacophore models, the generated models were screened against our prepared small database where the number of known active inhibitors were 65 and decoys were 106 and after screening, the receiver operating characteristic (ROC) curve (Figure 3) was generated.

The validated pharmacophore model of 1RO6 was used for getting the novel molecules from the databases. A total of 11590 molecules were generated during the first screening. Then based on specific pharmacophore fit value (45), we got 4048 molecules.

Molecular docking was carried out with three software simultaneously. All the molecules were docked to our predicted active site of the protein 1RO6. Initially, we docked the attached ligand rolipram with the protein. Then the molecules were docked. 145 molecules were docked in PyRx, Vega zz and AutoDock vina. and those molecules got selected that have a more binding score than rolipram.

Molecular dynamics (MD) simulation was carried out for 50 ns. Three important features known as RMSD (Root Mean Square Deviation), RMSF (Root Mean Square Fluctuation) and Rg (Radius of Gyration) were taken into account to check the relative stability of the ligands in the binding site of the protein.

Discussion

Figure 1 signifies the pharmacophore model of 1RO6. By analyzing the figure, it is seen that the pharmacophore model consists of 11 features. Among them, one is hydrophobic, two hydrogen bond acceptor and the remaining is exclusion volume. For hydrophobic feature PHE 446, TYR 233 AND ILE 410 residues are involved. GLN 443 is associated with the hydrogen bond acceptor feature.

From the receiver operating characteristic (ROC) (**figure 3**) curve that generated during the screening shows that the primary enrichment factor (EF%) was 2.6 with a good AUC (area under the ROC curve) value 1.0. This signifies that the pharmacophore model was capable of distinguishing between the true active and decoy molecules presented in the database. The remaining AUC was 1.0, 1.0 and 0.81 during the 5,10 and 100% of the database that screened while the EF was 2.6, 2.3 and 2.0 for 5, 10 and 100% screening of the database.

4048 molecules that remained after virtual screening were then filtered by applying the Lipinski's rules and ADMET. Finally, 145 molecules remained that satisfied the given criteria. That means all these molecules have the value of LogP less than 5, molecular weight less than 500, the number of hydrogen bond donors less than 5, the number of hydrogen bond acceptors less than 10 and the number of rotatable bonds less than 10. For ADMET properties, solubility, cytochrome

P450 (CYP450) 2D6 inhibition hepatotoxicity, HIA, plasma protein binding, AMES mutagenesis, PAINS were considered. The solubility range for all these molecules is between -1 to -5 which states that they have a good solubility property [47]. CYP2D6 and hepatotoxicity were 0 which means these molecules are less toxic and there is less chance of causing any interaction. Ames mutagenesis for all the molecules are negative which implies that the molecules don't have any mutagenic property [48]. The TPSA value for all the molecule was below 100 because TPSA value less than 100 increase the permeability of a molecule [49]. These 145 molecules were then taken for further study.

After molecular docking, these 145 molecules were filtered again. Binding affinity for rolipram was -8.4 kcal/mol in PyRx, -8.6 kcal/mol in Vega zz and -8.9 kcal/mol in AutoDock vina. From PyRx, 49 molecules remained having binding affinity more than -8.4 kcal/mol, 44 molecules from Vega zz possessing binding score more than -8.6 kcal/mol and 41 molecules from AutoDock vina having binding score more than -8.9 kcal/mol (**Table 1**). Finally, the molecules obtained from these three-docking programs were merged and got 21 molecules.

These 21 molecules were then taken for further filtration by rescoring. DrugScoreX (DSX) score of rolipram was set as standard and then sorted out molecules from 21 molecules. -17 kcal/mol was the score for rolipram. Out of 21 molecules, 9 molecules showed better score than rolipram (**Table 2**). We took these 9 molecules for further study.

In this part of research, 2D structure of the selected 9 molecules were generated (**Table 3**). 2D interaction of the potent inhibitors of the PDE4 shows that ASN B:395, GLN B:443, TYR B:233, ILE B:410, PHE B:446, ASP B:392 and THR B:407 was common among all these inhibitors [50]. In case of the selected molecule, those molecules were kept which were capable of interacting at least five key residues out of seven and it was seen that three molecules met the requirement. Finally, 3 molecules remained and these molecules were then subjected to MD simulation.

MD simulation technique is used to examine the stability of a chemical compound to its receptor site. The RMSD is considered an integral feature that implies the stability of the complex at the time of the simulation. For native protein, the overall RMSD was fluctuated between 0.4Å to 2.1Å. The RMSD value of the protein immediately reached to almost 2Å. After 3 ns the value gradually decreased and maintain a constant level up to 49 ns without any major fluctuation. RMSD reached to 2.1Å at the 50th ns of the simulation.

In the case of **CHEMBL3315249-protein** complex, the RMSD (**Figure 4**) fluctuation was very little and it was approximately from 0.4Å to 2.0Å during the whole simulation period. After starting the simulation, RMSD for this complex started to increased and reached 1.5Å after 4 ns and then started to decrease. This scenario continued for a very short period of time and finished after 10 ns. After 10 ns to 50 ns, this complex maintained a constant RMSD value with a very little fluctuation. On the other hand, the overall fluctuation for **CHEMBL3315269-protein** complex was between 0.4 Å to 1.8 Å. Immediately after starting the simulation, this complex maintained a constant level till 30 ns and during this time the RMSD value was below 1.6 Å. After 30ns, RMSD reached over 1.6Å which continued up to 40 ns. During this time, the fluctuation was too little. After 40th ns, RMSD reached to maximum value 1.8A and then decreased to 1.4Å and maintained the same level till the end of the simulation. For

complex **CHEMBL3315248-protein**, the overall value of RMSD was between 0.5Å to 2Å. At the beginning of the simulation, RMSD reached approximately 2Å then decreased immediately to 1.5Å and maintained this value till 40 ns with little bit variation. After 40th ns, RMSD started to increase gradually and reached to 2Å at 47th ns and then maintained this value till the end. Although there was a neglectable variation of the value during this period of simulation.

Radius of gyration (Rg) expresses the compactness of complex during the simulation. Rg of the native protein increased after the simulation began and stabilized after 9 ns. From 10th ns, it maintained a constant value till the end of the simulation with little bit fluctuation. For the **CHEMBL3315249-protein** complex, the Rg value range was from 21.2Å to 22.2Å (**Figure 5**). From the beginning of the simulation Rg value increased till 10 ns and then decreased. From 10th to 30th ns, Rg value was relatively stable. After 30 ns, Rg increased and reached to maximum value 22.2Å which persisted from 30 to 35 ns. After 35 ns, the value gradually decreased and maintained a stable state till the end of the simulation with negligible variation. **CHEMBL3315269-protein** had maximum Rg value of 21.9Å which was obtained approximately at the 5th ns. After 5 ns, the value gradually decreased and maintained a stable state during the whole simulation. Although approximately at the 37th ns, Rg was over 21.8Å but except this time, the value was below 21.8Å during the period. For **CHEMBL3315248-protein**, Rg began to increase from the beginning of the simulation and reached to 22A after 20 ns. Then the value decreased and maintained the level till 40th ns. At the 50th ns, Rg again reached to 22Å.

For RMSF value (**Figure 6**), **CHEMBL3315249-protein** complex and **CHEMBL3315269-protein** complex showed similarity with the native protein. There was no unusual fluctuation of the residues of protein-ligand complexes comparing to the non-liganded protein. Although **CHEMBL3315248-protein** complex showed a little bit higher fluctuation of the residues comparing the other two complexes.

After discussing the MD simulation result, it was seen that all the complex maintained a good stability during the whole simulation. RMSD value of the complexes indicates that all the ligands had good structural stability and strong intramolecular interaction with the residues during the whole simulation period. Rg value also indicates that they maintained a good structural compactness with the protein. On the other hand, **CHEMBL3315249-protein** complex and **CHEMBL3315269-protein** complex performed better than the **CHEMBL3315248-protein** complex in case of RMSF. From this MD simulation, it is clear that all the three molecules performed better in case of stability. Due to this, we took all these molecules as our final hit.

Conclusion

PDE4 is a novel target for the development of CNS acting drugs. In this research, pharmacophore-based virtual screening was carried out to get novel compounds. After multiple filtration three molecules were obtained. The purpose of this filtration was to remove the molecules that may be toxic. Finally, their stability was checked by molecular dynamic simulation study where all of them showed better stability with the protein. This is expected that this *in-silico* study will be helpful for the development of new molecules for Alzheimer's disease.

Acknowledgment

The author would like to express his gratitude to the Editor-in-chief and anonymous referees

for their careful reading and valuable suggestions which contribute to improve the exposition of the manuscript.

References

1. Wimo, A., Jönsson, L., Bond, J., Prince, M., Winblad, B., & International, A. D. (2013). The worldwide economic impact of dementia 2010. Alzheimer's & Dementia, 9(1), 1-11.
2. Houslay, M. D., & Milligan, G. (1997). Tailoring cAMP-signalling responses through isoform multiplicity. Trends in biochemical sciences, 22(6), 217-224.
3. Houslay, M. D., Sullivan, M., & Bolger, G. B. (1998). The multienzyme PDE4 cyclic adenosine monophosphate-specific phosphodiesterase family: intracellular targeting, regulation, and selective inhibition by compounds exerting anti-inflammatory and antidepressant actions. Advances in pharmacology (San Diego, Calif.), 44, 225-342.
4. Antoni, F. A. (2000). Molecular diversity of cyclic AMP signalling. Frontiers in neuroendocrinology, 21(2), 103-132.
5. Torphy, T. J. (1998). Phosphodiesterase isozymes: molecular targets for novel antiasthma agents. American Journal of Respiratory and Critical Care Medicine, 157(2), 351-370.
6. Hansen, G., Jin, S. L. C., Umetsu, D. T., & Conti, M. (2000). Absence of muscarinic cholinergic airway responses in mice deficient in the cyclic nucleotide phosphodiesterase PDE4D. Proceedings of the National Academy of Sciences, 97(12), 6751-6756.
7. Soderling, S. H., & Beavo, J. A. (2000). Regulation of cAMP and cGMP signaling: new phosphodiesterases and new functions. Current opinion in cell biology, 12(2), 174-179.
8. Beavo, J. A., & Brunton, L. L. (2002). Cyclic nucleotide research—still expanding after half a century. Nature reviews Molecular cell biology, 3(9), 710.
9. Mehats, C., Andersen, C. B., Filopanti, M., Jin, S. C., & Conti, M. (2002). Cyclic nucleotide phosphodiesterases and their role in endocrine cell signaling. TRENDS in Endocrinology & Metabolism, 13(1), 29-35.
10. Conti, M., & Jin, S. L. C. (1999). The molecular biology of cyclic nucleotide phosphodiesterases. In Progress in nucleic acid research and molecular biology (Vol. 63, pp. 1-38). Academic Press.
11. Bolger, G. B., McPhee, I., & Houslay, M. D. (1996). Alternative Splicing of cAMP-specific Phosphodiesterase mRNA Transcripts CHARACTERIZATION OF A NOVEL TISSUE-SPECIFIC ISOFORM, RNPDE4A8. Journal of Biological Chemistry, 271(2), 1065-1071.
12. Wachtel, H. (1983). Potential antidepressant activity of rolipram and other selective cyclic adenosine 3′, 5′-monophosphate phosphodiesterase inhibitors. Neuropharmacology, 22(3), 267-272.
13. MIZOKAWA, T., KIMURA, K., IKOMA, Y., Kimio, H. A. R. A., OSHINO, N., YAMAMOTO, T., & Showa, U. E. K. I. (1988). The effect of a selective phosphodiesterase inhibitor, rolipram, on muricide in olfactory bulbectomized rats. Japanese journal of pharmacology, 48(3), 357-364.
14. Blokland, A., Schreiber, R., & Prickaerts, J. H. H. J. (2006). Improving

memory: a role for phosphodiesterases. Current pharmaceutical design, 12(20), 2511-2523.

15. Parkes, J. D., Thompson, C., Brennan, L., Gajraj, N., Howcroft, B., & Ruiz, J. (1984). Rolipram in Parkinson's disease. Advances in neurology, 40, 563-565.

16. Yang, L., Calingasan, N. Y., Lorenzo, B. J., & Beal, M. F. (2008). Attenuation of MPTP neurotoxicity by rolipram, a specific inhibitor of phosphodiesterase IV. Experimental neurology, 211(1), 311-314.

17. Huai, Q., Wang, H., Sun, Y., Kim, H. Y., Liu, Y., & Ke, H. (2003). Three-dimensional structures of PDE4D in complex with roliprams and implication on inhibitor selectivity. Structure, 11(7), 865-873.

18. Güner, O. F., & Bowen, J. P. (2014). Setting the record straight: the origin of the pharmacophore concept. Journal of chemical information and modeling, 54(5), 1269-1283.

19. Kalyaanamoorthy, S., & Chen, Y. P. P. (2011). Structure-based drug design to augment hit discovery. Drug discovery today, 16(17-18), 831-839.

20. Fredholm, B. B., Abbracchio, M. P., Burnstock, G., Daly, J. W., Harden, K. T., Jacobson, K. A., ... & Williams, M. (1994). VI. Nomenclature and classification of purinoceptors. Pharmacological reviews, 46(2), 143.

21. Yang, S. Y. (2010). Pharmacophore modeling and applications in drug discovery: challenges and recent advances. Drug discovery today, 15(11-12), 444-450.

22. Muchtaridi, M., Syahidah, H., Subarnas, A., Yusuf, M., Bryant, S., & Langer, T. (2017). Molecular docking and 3D-pharmacophore modeling to study the interactions of chalcone derivatives with estrogen receptor alpha. Pharmaceuticals, 10(4), 81.

23. Meng, X. Y., Zhang, H. X., Mezei, M., & Cui, M. (2011). Molecular docking: a powerful approach for structure-based drug discovery. Current computer-aided drug design, 7(2), 146-157.

24. Wolber, G., & Langer, T. (2005). LigandScout: 3-D pharmacophores derived from protein-bound ligands and their use as virtual screening filters. Journal of chemical information and modeling, 45(1), 160-169.

25. Guariento, S., Bruno, O., Fossa, P., & Cichero, E. (2016). New insights into PDE4B inhibitor selectivity: CoMFA analyses and molecular docking studies. Molecular diversity, 20(1), 77-92.

26. Mysinger, M. M., Carchia, M., Irwin, J. J., & Shoichet, B. K. (2012). Directory of useful decoys, enhanced (DUD-E): better ligands and decoys for better benchmarking. Journal of medicinal chemistry, 55(14), 6582-6594.

27. Desai, P. V., Patny, A., Sabnis, Y., Tekwani, B., Gut, J., Rosenthal, P., ... & Avery, M. (2004). Identification of novel parasitic cysteine protease inhibitors using virtual screening. 1. The ChemBridge database. Journal of medicinal chemistry, 47(26), 6609-6615.

28. Schulz, M. N., Landström, J., Bright, K., & Hubbard, R. E. (2011). Design of a fragment library that maximally represents available chemical

space. Journal of computer-aided molecular design, 25(7), 611.

29. Kirchmair, J., Wolber, G., Laggner, C., & Langer, T. (2006). Comparative performance assessment of the conformational model generators omega and catalyst: a large-scale survey on the retrieval of protein-bound ligand conformations. Journal of chemical information and modeling, 46(4), 1848-1861.

30. Lipinski, C. A. (2004). Lead-and drug-like compounds: the rule-of-five revolution. Drug Discovery Today: Technologies, 1(4), 337-341.

31. Lagorce, D., Bouslama, L., Becot, J., Miteva, M. A., & Villoutreix, B. O. (2017). FAF-Drugs4: free ADME-tox filtering computations for chemical biology and early stages drug discovery. Bioinformatics, 33(22), 3658-3660.

32. Berman, H., Henrick, K., Nakamura, H., & Markley, J. L. (2006). The worldwide Protein Data Bank (wwPDB): ensuring a single, uniform archive of PDB data. Nucleic acids research, 35(suppl_1), D301-D303.

33. Seeliger, D., & de Groot, B. L. (2010). Ligand docking and binding site analysis with PyMOL and Autodock/Vina. Journal of computer-aided molecular design, 24(5), 417-422.

34. Chen, I. J., & Foloppe, N. (2010). Drug-like bioactive structures and conformational coverage with the LigPrep/ConfGen suite: comparison to programs MOE and catalyst. Journal of chemical information and modeling, 50(5), 822-839.

35. Dallakyan, S., & Olson, A. J. (2015). Small-molecule library screening by docking with PyRx. In Chemical biology (pp. 243-250). Humana Press, New York, NY.

36. Mazzolari, A., Vistoli, G., Testa, B., & Pedretti, A. (2018). Prediction of the Formation of Reactive Metabolites by A Novel Classifier Approach Based on Enrichment Factor Optimization (EFO) as Implemented in the VEGA Program. Molecules, 23(11), 2955.

37. Trott, O., & Olson, A. J. (2010). AutoDock Vina: improving the speed and accuracy of docking with a new scoring function, efficient optimization, and multithreading. Journal of computational chemistry, 31(2), 455-461.

38. Gohlke, H., Hendlich, M., & Klebe, G. (2000). Knowledge-based scoring function to predict protein-ligand interactions. Journal of molecular biology, 295(2), 337-356.

39. Krieger, E., & Vriend, G. (2015). New ways to boost molecular dynamics simulations. Journal of computational chemistry, 36(13), 996-1007.

40. Krieger, E., Koraimann, G., & Vriend, G. (2002). Increasing the precision of comparative models with YASARA NOVA—a self-parameterizing force field. Proteins: Structure, Function, and Bioinformatics, 47(3), 393-402.

41. Krieger, E., Nielsen, J. E., Spronk, C. A., & Vriend, G. (2006). Fast empirical pKa prediction by Ewald summation. Journal of molecular graphics and modelling, 25(4), 481-486.

42. Dickson, C. J., Madej, B. D., Skjevik, Å. A., Betz, R. M., Teigen, K., Gould, I. R., & Walker, R. C. (2014). Lipid14: the amber lipid force field. Journal of chemical theory and computation, 10(2), 865-879.

43. Maier, J. A., Martinez, C., Kasavajhala, K., Wickstrom, L., Hauser, K. E., & Simmerling, C. (2015). ff14SB: improving the accuracy of protein side chain and backbone parameters from ff99SB. Journal of chemical theory and computation, 11(8), 3696-3713.

44. Stewart, J. J. (1990). MOPAC: a semiempirical molecular orbital program. Journal of computer-aided molecular design, 4(1), 1-103.

45. Wang, J., Wolf, R. M., Caldwell, J. W., Kollman, P. A., & Case, D. A. (2004). Development and testing of a general amber force field. Journal of computational chemistry, 25(9), 1157-1174.

46. Seidel, T., Bryant, S. D., Ibis, G., Poli, G., & Langer, T. (2017). 3D pharmacophore modeling techniques in computer-aided molecular design using LigandScout. Tutorials Chemoinform, 281, 279-309.

47. Lusci, A., Pollastri, G., & Baldi, P. (2013). Deep architectures and deep learning in chemoinformatics: the prediction of aqueous solubility for drug-like molecules. Journal of chemical information and modeling, 53(7), 1563-1575.

48. Ames, B. N., McCann, J., & Yamasaki, E. (1975). Methods for detecting carcinogens and mutagens with the Salmonella/mammalian-microsome mutagenicity test. Mutation Research/Environmental Mutagenesis and Related Subjects, 31(6), 347-363.

49. Pajouhesh, H., & Lenz, G. R. (2005). Medicinal chemical properties of successful central nervous system drugs. NeuroRx, 2(4), 541-553.

50. 50.Çifci, G., Aviyente, V., & Akten, E. D. (2012). Molecular Docking Study Based on Pharmacophore Modeling for Novel PhosphodiesteraseIV Inhibitors. Molecular informatics, 31(6-7), 459-471.

Molecules ID	PyRx (kcal/mol)	Vega zz (kcal/mol	AutoDock vina (kcal/mol)
CHEMBL1417438	-9.1	-8.8	-9.2
CHEMBL3315249	-8.9	-8.8	-9.2
CHEMBL1558592	-9.9	-9.5	-9.8
CHEMBL1782297	-9.7	-9.6	9.4
CHEMBL1782286	-9.1	-8.9	-9.5
CHEMBL1782296	-9.2	-9.1	-9.3
CHEMBL3315269	-9.6	-9.2	-9.5
CHEMBL1784111	-8.9	-8.6	-9.1
CHEMBL1784109	-9.0	-8.8	-9.3
CHEMBL3315248	-8.6	-8.8	-9.1
CHEMBL1304937	-8.9	-8.7	-9.2
CHEMBL1495549	-8.5	-8.8	-9.0
CHEMBL1366677	-8.5	-8.7	-9.2
CHEMBL3315263	-8.9	-9.0	-9.1
CHEMBL1434873	-9.1	-8.9	-9.3
CHEMBL3315247	-8.7	-8.8	-9.0
CHEMBL1358651	-8.6	-8.9	-9.2
CHEMBL1406744	-9.0	-8.9	-9.3
CHEMBL1454872	-8.9	-9.0	-9.3
CHEMBL3114935	-8.8	-8.9	-9.4
CHEMBL1597216	-8.7	-8.8	-9.0
Rolipram	-8.4	-8.6	-8.9

Table 1: Molecular docking score of the selected molecules and rolipram

Molecules ID	DSX scoring
CHEMBL3315248	-20
CHEMBL3315247	-21
CHEMBL3315269	-18
CHEMBL1597216	-19
CHEMBL3315249	-22
CHEMBL1558592	-18
CHEMBL1782297	-19
CHEMBL1782286	-21
CHEMBL1782296	-18
Rolipram	-17

Table 2: DSX scoring of the molecules and rolipram

Molecules	Hydrogen bonding	Hydrophobic interaction	Van der Waals
CHEMBL3315249	ASN B:283, GLU B:304, GLN B:443	**Pi-pi Stacked**: PHE B:446, TYR B:233, PHE B:414 Pi-pi T-shaped: TYR B:233, PHE B:446 **Alkyl**: MET B:347, ILE B:410, MET B:431 **Pi-alkyl**: ILE B:410, MET B:431	HIS B:278, SER B:282, LEU B:303, GLN B:284, HIS B:234, ILE B:450, SER B:442. TRP B:406, TYR B:403, THR B:407, ASN B:395
CHEMBL3315269	TYR B:233, HIS B:278	**Unfavorable acceptor-acceptor:** ASP B:275 **Pi-pi Stacked**: MET B:431, PHE B:446 **Pi-Sulfur**: MET B:431 **Pi-Cation**: ASP B:392, HIS B:234 **Pi-Anion**: ASP B:393 Alkyl: ILE B:410, TYR B:403 **Pi-alkyl**: ILE B:410, PHE B:446	PRO B:396, THR B:407, ASN B:395, TRP B:406, GLN B:443, SER B:442, PHE B:414, MET B:347, THR B:345, GLU B:304, HIS B:307, HIS B:238, LEU B:393
CHEMBL3315248	HIS B:278, ASN B:395	**Pi-pi Stacked**: PHE B:446, PHE B:414 **Alkyl**: ILE B:410, LEU B:303 **Pi-alkyl**: CYS B:432 Pi-Cation: HIS B:234	VAL B:281, GLN B:417, SER B:282, PRO B:396, THR B:407, TRP B:406, GLN B:443, TYR B:233, LEU B:393, MET B:347, THR B:345, ASP B:275, GLU B:304, HIS B:307, HLU B:413
Rolipram	HIS B:234, GLN B:443	**Pi-pi Stacked:** TYR B:233, PHE B:446 **Pi-pi T-shaped:** TYR B:233, PHE B:446 **Alkyl:** MET B:431, PHE B:414 **Pi-alkyl:** ILE B:410, PHE B:446	HIS B:238, ASN B:395, TRP B:406, TYR B:403, THR B:407, MET B:411, SER B:442, LEU B:393, MET B:347, ASP B:392

Table 3: Interaction of the selected ligands and rolipram with the residues of the protein

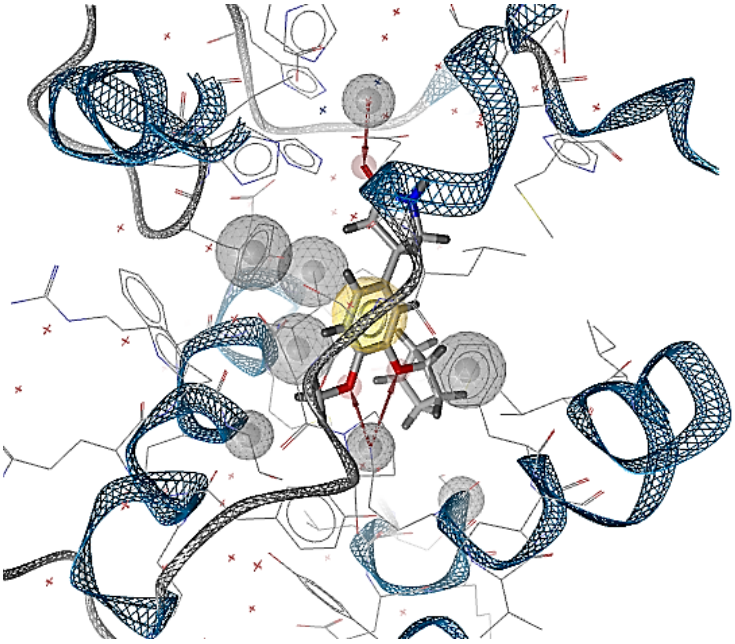

Figure 1: Pharmacophore model of 1RO6

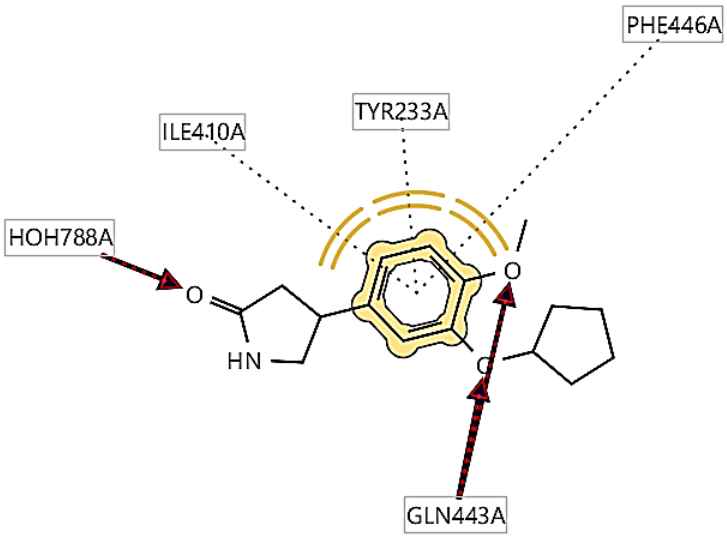

Figure 2: 2D structure of the attached ligand with 1RO6

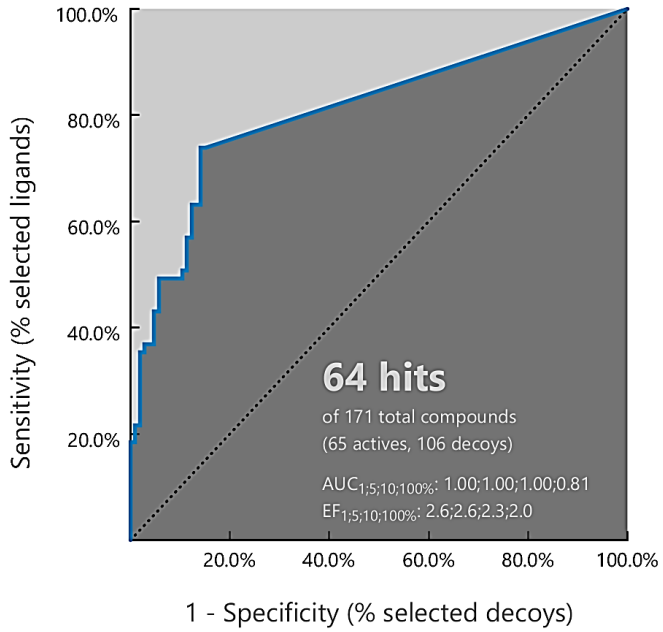

Figure 3: ROC curve obtained during the screening of the database

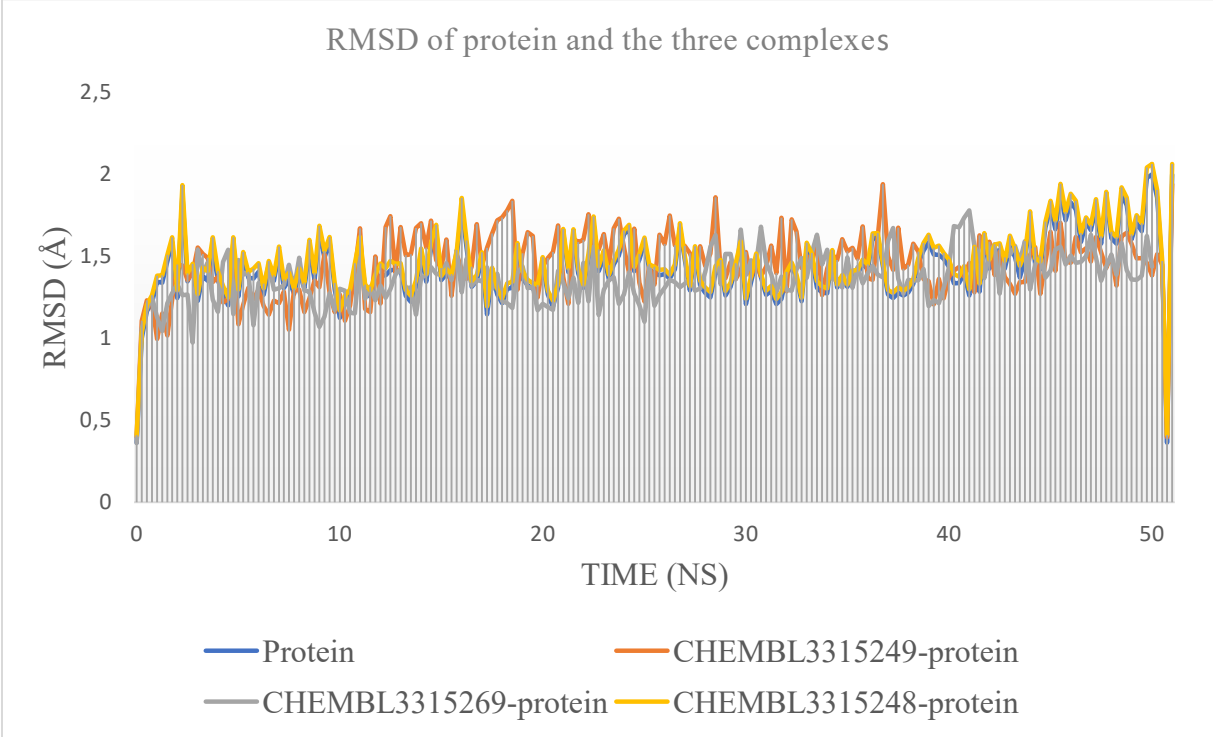

Figure 4: RMSD value of the ligand-protein complex and the protein

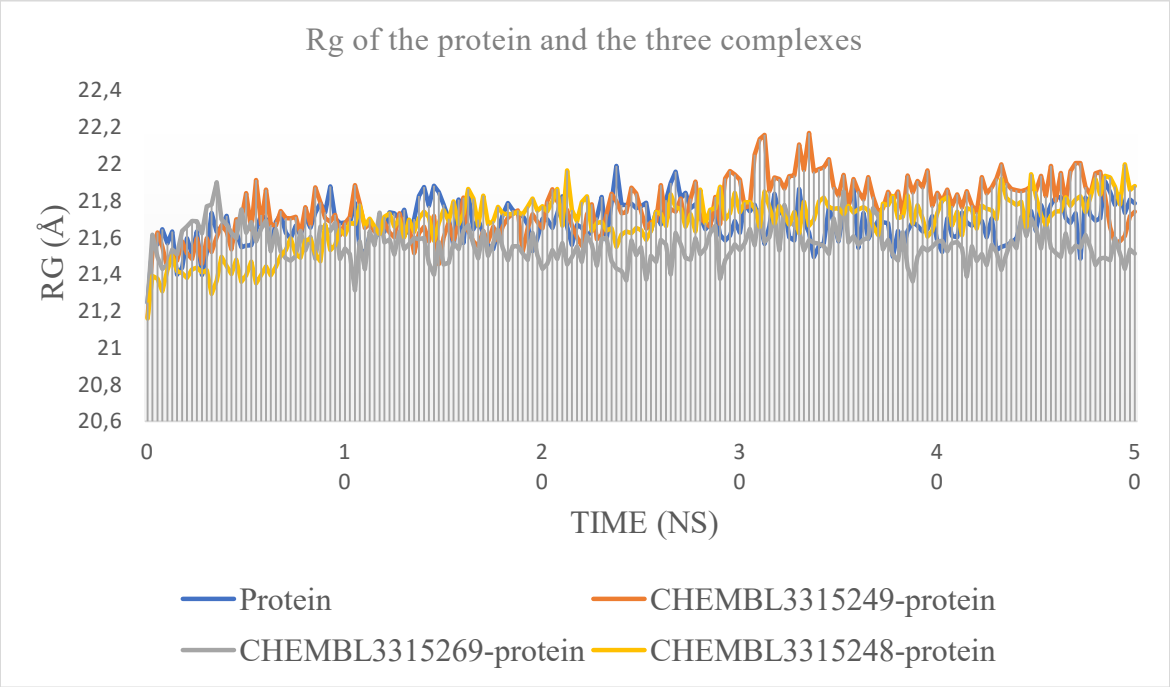

Figure 5: Rg value of the ligand-protein complexes and the protein

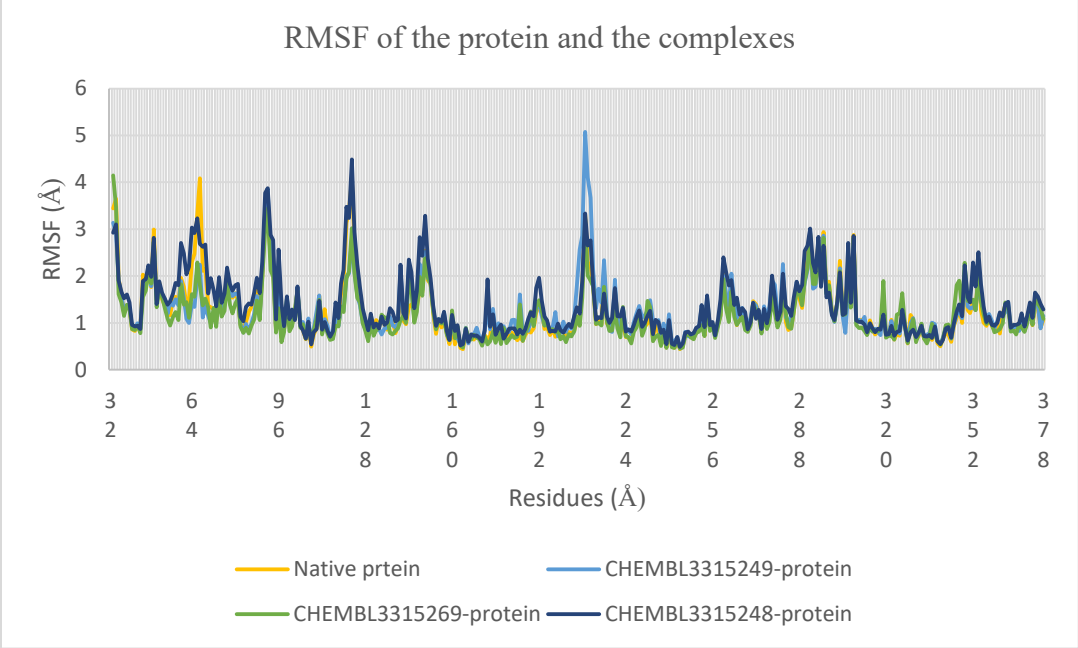

Figure 6: RMSF value of the ligand-protein complexes and protein